

Synthesis of Niobium Doped ZnO Nanoparticles by Electrochemical Method: Characterization, Photodegradation of Indigo Carmine Dye and Antibacterial Study

Rakesh¹, Sannaiah Ananda¹, Netkal M. Made Gowda², Kithanakere Ramesh Raksha¹

¹Department of Studies in Chemistry, University of Mysore, Mysore, India

²Department of Chemistry, Western Illinois University, One University Circle, Macomb, USA

Email: rakesh_chemin@yahoo.com, snananda@yahoo.com, gn-made@wiu.edu

Received 19 June 2014; revised 13 August 2014; accepted 3 September 2014

Copyright © 2014 by authors and Scientific Research Publishing Inc.

This work is licensed under the Creative Commons Attribution International License (CC BY).

<http://creativecommons.org/licenses/by/4.0/>



Open Access

Abstract

Niobium doped Zinc oxide nanoparticles has been synthesized through electrochemical method and characterized by UV-Visible spectroscopy, IR Spectroscopy, SEM, XRD, ICPMS and EDAX data. The UV-Visible spectroscopy result reveals that the band gap energy of ZnO/Nb₂O₅ nanoparticles to be 3.8 eV. The XRD results show that the crystallite size is to be 31.9 nm. The ICPMS data indicate the presence of 3,3461,328 counts of 93 Nb and 577,906,390 counts of 66 Zn. An improvement in the photocatalytic degradation of Indigocarmine dye (IC) in comparison to commercially available pure ZnO was observed. The photodegradation efficiency for ZnO/Nb₂O₅ and ZnO were found to be 97.4% and 52.1% respectively. The enhancement in photocatalytic activity of ZnO/Nb₂O₅ was ascribed to the extended light absorption range and suppression of electron hole pair recombination upon Nb loading. The antibacterial activity of ZnO/Nb₂O₅ nanoparticles was investigated. These particles were shown to have an effective bactericide.

Keywords

ZnO/Nb₂O₅ Nanoparticles, Electrochemical Method, Niobium Coated Platinum Electrode (Pt/Nb), Indigo Carmine Dye (IC), *E. coli*

1. Introduction

ZnO is a wide-band gap oxide semiconductor with a direct energy gap of about 3.37 eV, and as a consequence it

How to cite this paper: Rakesh, Ananda, S., Gowda, N.M.M. and Raksha, K.R. (2014) Synthesis of Niobium Doped ZnO Nanoparticles by Electrochemical Method: Characterization, Photodegradation of Indigo Carmine Dye and Antibacterial Study. *Advances in Nanoparticles*, 3, 133-147. <http://dx.doi.org/10.4236/anp.2014.34018>

absorbs UV radiation due to the band-to-band transitions [1]. Recently, ZnO has attracted growing attention due to its potential applications, such as in ultra-violet light emitting devices and laser devices [2]. Furthermore, ZnO is an environmentally friendly material, in this process, irradiation of semiconductor particles with sufficiently energetic light results in the formation of electron-hole pairs, which can subsequently migrate to the particle surface and react with adsorbed molecules to generate free radicals. These free radicals are highly reactive and can therefore mineralize organic pollutants into harmless compounds, such as CO₂, H₂O and simple mineral salts [3]-[5].

ZnO is known to be one kind of the important photo catalysts because of its unique advantages, such as its low price, high photocatalytic activity and nontoxicity, that has attracted a great deal of attention with respect to the degradation of various pollutant due to its high photosensitivity and stability [6]. Among these properties, the degradation of the pollutants catalysed by ZnO has been studied widely [7]. It has also suggested that ZnO is a low cost alternative photocatalyst to TiO₂ for photodegradation of organics in aqueous solutions [8] [9], as it has a similar band gap energy (3.37 eV) [10] with higher photocatalyst efficiencies was reported [11] [12]. However, the photocatalyst properties of ZnO for the degradation of pollutant are directly related to their preparation e.g.: particle size, morphology and dopant concentrations.

Electrochemical method is a cost effective and versatile process for controlling the production of nanoparticle materials. This process has been demonstrated as one step, suitable for dry synthesis of high surface area, and highly efficient for noble metal laden catalysts. These advantages of electrochemical method promoted us to apply for production of Nb-loaded ZnO nanoparticles for photocatalyst in photodegradation of various organic solution. The presence of the loading metal ions/metal oxide in the ZnO crystalline matrix significantly affects the photocatalytic activity, charge carriers recombination rate and interfacial electron transfer rate [13]. Generally speaking, the metal ions used as dopants are often the transition metal ions, e.g.: Co [14], Mn [15], T [16], La [17], Fe [18], Ni [19], N [20] and so forth. However, no previous work has been reported on the photocatalytic photodegradation of organic contaminants by Nb-loaded ZnO NPs. In present article, we synthesized and report on the photocatalytic degradation behaviour of Indigo carmine on Nb-loaded ZnO nanoparticles under UV-irradiation.

2. Experimental

All chemicals used were of the analytical grades of purity, niobium chloride was purchased from Alfa Aesar, Indigo carmine dye from Merck, Zinc metal wire from Alfa Aesar. All solutions were prepared in double distilled water. Absorption spectra was recorded on UV-Visible spectrophotometer (Shimadzu-1700 series). The FTIR spectra was recorded on Shimadzu IR-affinity-1 by dispersing the nanomaterial in KBr (0.3 wt%). The crystallographic interpretations were performed by X-ray diffractometer (Panalytical X-pert) using Cu α wavelength ($\lambda = 1.5406$) and scanning range from 23° to 103.9°. The morphological feature of the semiconductor under study was determined by scanning electron microscopy (ZEISS model). The elemental analysis for the confirmation of loading of Niobium to Zinc oxide is conformed from Energy dispersive X-ray analysis (EDAX) and Inductively coupled plasma mass spectroscopy ICPMS (Thermo scientific X-series 2).

2.1. Electrochemical Synthesis of ZnO/Nb₂O₅ Nanoparticles

In this method a thin film of niobium was deposited electrochemically on a platinum electrode (Pt/Nb) from niobium chloride solution (0.1 M). The preparation of ZnO/Nb₂O₅ nanoparticles were carried in a reaction chamber containing 20 ml of NaHCO₃ (0.5%) solution. Voltage power supply of 15 V, current of 22 mA and (Pt/Nb) electrode/Zinc wire as anode and Pt electrode as cathode were used. The experiment was run until the complete dissolution of niobium from the platinum plate at constant temperature. The anodic dissolution of Zn and Nb gives Zn(II) and Nb(V) ions which are electrochemically reacted with aqueous NaHCO₃ (0.5%) to form Zn(II) oxides/hydroxide with Nb(V) oxide. The solid obtained was washed with double distilled water till complete removal of unreacted NaHCO₃. The wet powder was then dried at a temperature 250°C - 400°C for dehydration and removal of hydroxides to get ZnO/Nb₂O₅. The synthesis takes place at the electrodes-electrode interface or close to the electrode within electrical double layer [21]. The product is deposited on the electrode in the form of thin film or coating and also it floats in the electrolyte solution which is collected by filtration [22]. The pH of the solution before electrolysis was found to be 9.0 which becomes much more alkaline (9.6) after electrolysis because of the formation of alkali (NaOH). The rate of electrochemical reaction is not same for all the metals, as

the redox potential of Zn (-0.7618 v) and Nb (-1.099 v) is different. Since the dissolution potential for Nb is more negative than Zn, it is expected that the formation of Nb₂O₅ takes place in competition with the formation of ZnO. Hence the product would be ZnO/Nb₂O₅ nanoparticle oxide. The electrochemical reaction takes place according to the following mechanism (Scheme 1).

2.2. Determination of Photocatalytic Activities

Indigo carmine dye (Molecular formulae: C₁₆H₈O₈N₂S₂, Molecular weight: 466.16, λ_{max} = 610 nm) solution of (1 × 10⁻⁴ M) was prepared by dissolving in distilled water. This solution was then used as a test contaminant for investigating photocatalytic activities of the commercial ZnO and ZnO/Nb₂O₅ nanoparticles. The evaluation was carried out both under UV light and Sunlight in order to investigate the efficiency of commercial ZnO and ZnO/Nb₂O₅ nanoparticles. To examine the photocatalytic activity 5.0 ml of colloidal solution upon exposure to light for equal interval of time were transferred to centrifuge tubes and centrifuged at 800 rpm to remove the dispersed catalyst and percent transmission was recorded for the colour solution. Chemical oxygen demand (COD) was estimated before and after treatment using dichromate oxidation method [23]. The increase in percent transmission and decrease in COD (mg/l) of dye solution with colour removal was observed to be more in ZnO/Nb₂O₅ compared to commercial ZnO material.

3. Results and Discussion

3.1. Uv-Visible Spectra

Uv-Visible spectrum (Figure 1) of ZnO/Nb₂O₅ over the range 200 - 800 nm showed photoabsorption properties no longer than 240 nm, which suggest that the catalyst is photo active under UV light irradiation. Assuming the

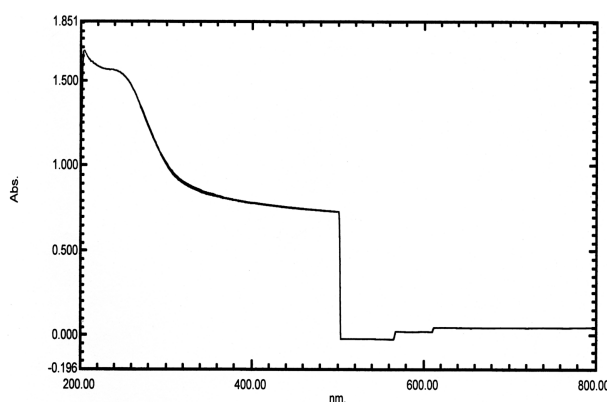
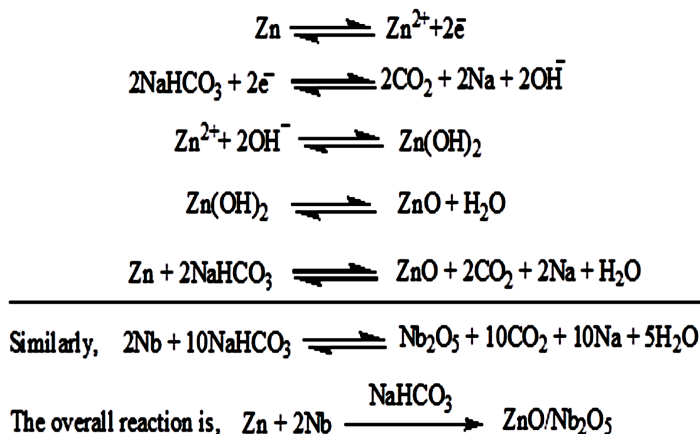


Figure 1. Uv-Vis spectrum of ZnO/Nb₂O₅.



Scheme 1. Probable mechanism for synthesis of ZnO/Nb₂O₅ nanoparticles.

ZnO/Nb₂O₅ solid asdirect semiconductor and it is possible to calculate the band gap of ZnO/Nb₂O₅ by constructing a Tauc plot [24]. The Tauc plot of ZnO/Nb₂O₅ is displayed in **Figure 2**. The energy of the band gap could be thus estimated to be 3.8 eV for ZnO/Nb₂O₅. ZnO/Nb₂O₅ is slightly greyish in colour. It is reported that Nb loading results in enlarge surface area of the Nb-loaded ZnO photocatalyst. However, the increase of surface area is likely not the main factor affecting the photocatalytic activity of Nb-loaded ZnO. Other factor that could affect photocatalytic efficiency are such as availability of active sites, crystalline structure, pore size and number/nature of trapped sites [25] [26]. According to the literatures and the fact that niobium acting as an electron trap [27], an enhanced photocatalytic activity of Nb-loaded ZnO nanoparticles found in our study was likely ascribed to a decrease of electron-hole pair recombination and thus promoting the photocatalytic activity [28].

3.2. Infrared Spectra

Figure 3 represents the IR spectrum of the ZnO/Nb₂O₅ nanoparticles. Metal oxides generally give absorption bands below 1000 cm⁻¹ arising from interatomic vibrations. A band around 450 cm⁻¹ corresponds to Zn-O bonds. A peak at 708 cm⁻¹ and 941cm⁻¹ corresponds to Nb-O bending and stretching vibrations. The peak at 1120 cm⁻¹ indicates the formation of ZnO. A peak at 2360 cm⁻¹ corresponds to the absorbed of CO₂ on the metallic cations.

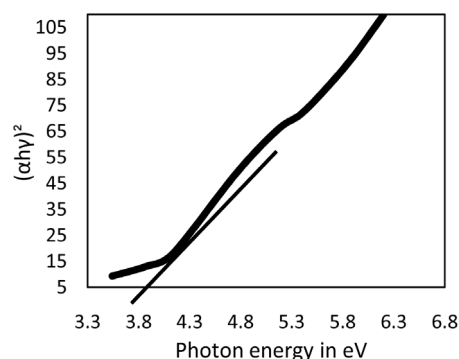


Figure 2. Tauc plot of ZnO/Nb₂O₅.

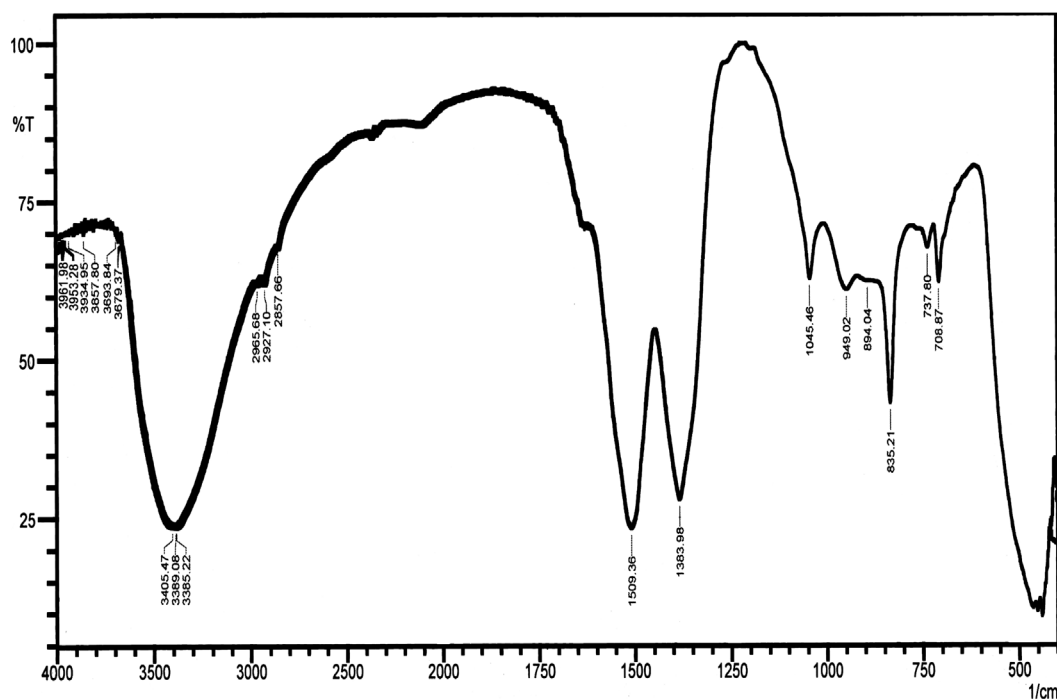


Figure 3. IR spectra of ZnO/Nb₂O₅ nanoparticles.

A peak at 1630 cm^{-1} and $3500 - 3800\text{ cm}^{-1}$ indicates the presence of water molecules and hydroxyl radicals respectively on the surface of the ZnO/Nb₂O₅ nanoparticles. The M-O frequencies observed for nanoparticles of metal oxides are in accordance with literature values [29].

3.3. X-Ray Diffraction

XRD pattern of ZnO/Nb₂O₅ is shown in Figure 4, it exhibits dominant diffraction peaks. The (hkl) values according to Treor programming (IUCR) of the peaks 28.15° , 31.88° , 34.4° , 36.2° , 47.5° , 58.2° , 62.8° and 67.9° corresponds to the crystal planes of (111), (201), (020), (310), (320), (222), (330) and (511) respectively. The crystallite size of ZnO/Nb₂O₅ was found to be 31.9 nm, the unit cell volume is 334 \AA^3 , and $\alpha = \gamma = 90^\circ \neq \beta$, $a \neq b \neq c$, ($a = 10.39\text{ \AA}$, $b = 5.203\text{ \AA}$, $c = 7.608\text{ \AA}$). Accordingly ZnO/Nb₂O₅ belongs to monoclinic crystal system. The diffraction peaks at 28.15° , 36.2° , and 58.2° corresponds to Nb phase are seen in XRD pattern of ZnO/Nb₂O₅ nanoparticles which confirms the presence of Nb (V) in ZnO matrix [30].

3.4. Inductively Coupled Plasma-Mass Spectroscopy

The elemental analysis of ZnO/Nb₂O₅ nanoparticles was carried out using Thermo scientific-X-series 2 with plasma lab software. The results shows the loading of niobium to the zinc oxide matrix in terms of atomic counts, where 50.0 mg of nanoparticles were dissolved in 50 ml of 2% HNO₃ solution and the above solution was aspirated to the instrument after the blank analysis. The analysis was carried out in triplet and atomic count, mean and % RSD has been tabulated in Table 1.

Thus the above data confirms the presence of Niobium in ZnO matrix. The instrument parameters used for performing the analysis is shown in Table 2.

Table 1. ICP-MS results for the loading of Niobium to ZnO matrix.

Run	66 Zn	93 Nb
1	572875130.00	33040528.00
2	574806010.00	33201860.00
3	586038030.00	34141598.00
X	577906390.00	33461328.00
σ	7108077.900	594627.530
%RSD	1.230	1.777

Table 2. Instrumental parameters for the analysis of ZnO/Nb₂O₅.

Plasma gas flow	13.0 liter/minute
Auxiliary gas flow	0.7 liter/Minute
Nebulizer pressure	0.9 bar
Pump speed	40 rpm
Sample uptake delay	30 seconds
Plasma power	1.4 Kw
Nebulizer	Concentric
Acquisitiontime (Dwell time)	30 milli seconds/channel
Number of channel	3
Channel spacing	0.02 Amu

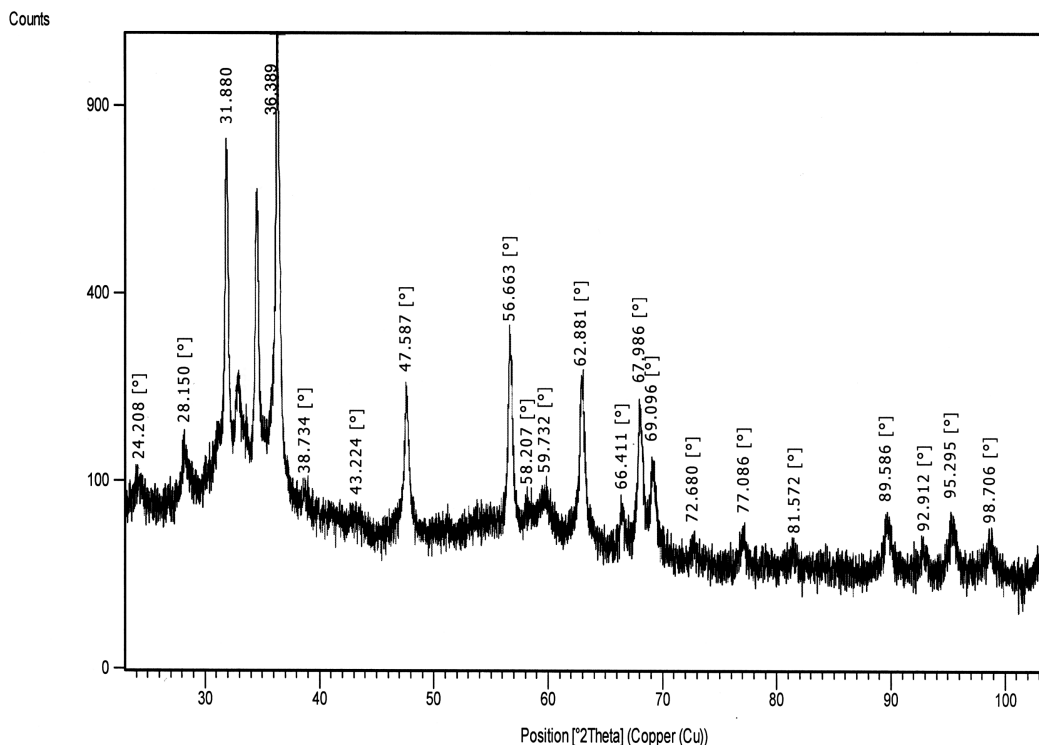


Figure 4. XRD pattern of ZnO/Nb₂O₅ nanoparticles.

3.5. Scanning Electron Microscopy (SEM)

Scanning electron microscopy was used to study the surface morphology of ZnO/Nb₂O₅ nanoparticles. A scanning electron microscope (ZESIS) was employed to characterize the sample. A numerous nanorods with bundle-like structures were formed as depicted in **Figure 5**. These nanorods lies close to each other and their lengths upto several micrometres.

3.6. Energy Dispersive X-Ray Analysis

The elemental analysis of the ZnO/Nb₂O₅ nanoparticles was carried out using EDAX (JOEL, JED-2300, Germany). The EDAX analysis shows presence of only Zn, Nb and O as expected, no other impurity elements were present in the ZnO/Nb₂O₅ nanoparticles (**Figure 6**).

The mass% of Zn and O in sample was not as per stoichiometric proportion. The entire sample were observed to be oxygen deficient. The deficiency or excess of the constituent material results in distorted band structure with corresponding increase in conductivity. Zinc oxide loses oxygen on heating so that the zinc is in excess. The oxygen of course evolves as electrically neutral substance so that it is associated with each excess zinc ion in the crystal; there will be two electrons that remain trapped in the solid material, thus leading to non-stoichiometricity in the solid. This leads to the formation of the semiconducting nature of the material [31].

4. Photodegradation and COD Measurements

The percent transmission of dye solution in presence of ZnO/Nb₂O₅ at different intervals of time is much higher as compared to solutions with ZnO. Thus, photocatalytic degradation is favourably affected by ZnO/Nb₂O₅ (**Figure 7**). A plot of log T versus time is linear, hence the reaction follows pseudo first order kinetics. The rate of photodegradation for ZnO/Nb₂O₅ was observed to be $9.67 \times 10^{-5} \text{ sec}^{-1}$ (~97% reaction) which is higher than the value obtained for ZnO $5.77 \times 10^{-5} \text{ sec}^{-1}$.

4.1. Effect of Concentration of Indigo Carmine Dye

The reaction was performed with different concentrations of Indigo carmine with constant weight of ZnO/Nb₂O₅

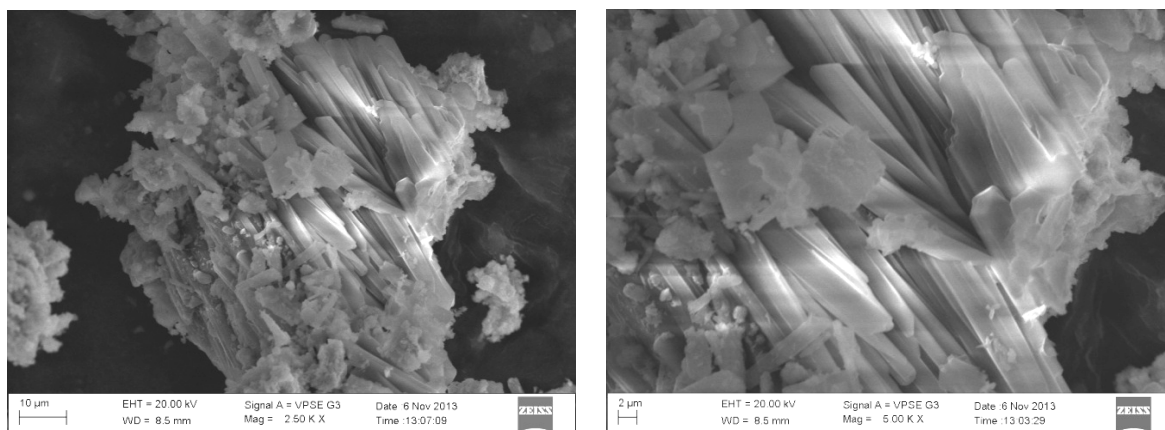


Figure 5. SEM images of ZnO/Nb₂O₅ nanoparticles.

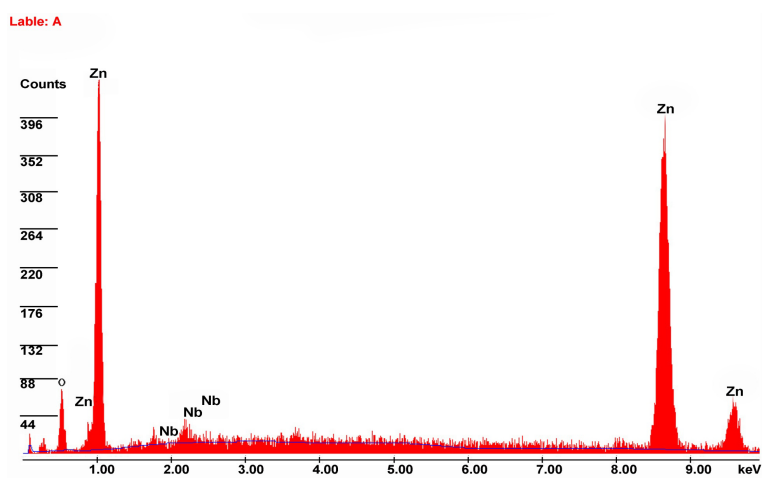


Figure 6. EDAX spectra of ZnO/Nb₂O₅ nanoparticles.

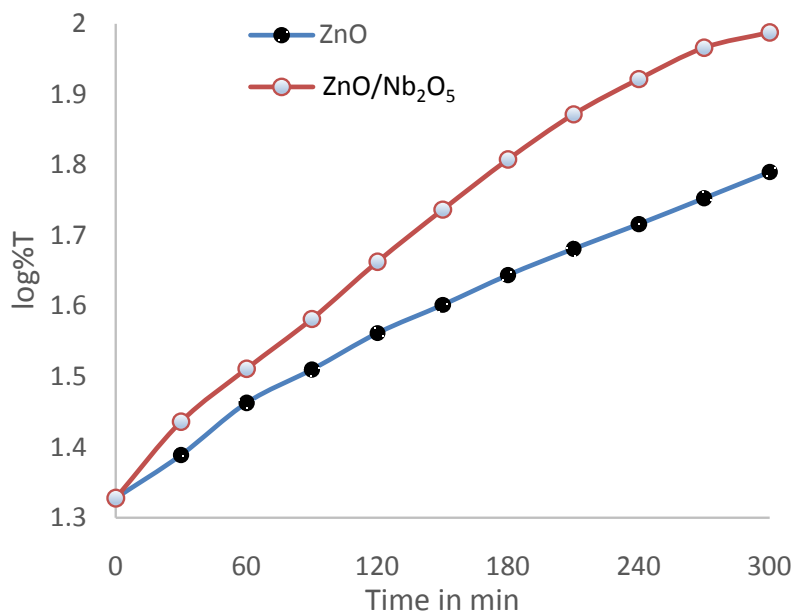


Figure 7. Photodegradation kinetics of indigo carmine dye.

catalyst. The change in concentration of the Indigo carmine was recorded by change in colour using Spectrophotometer. A plot of $\log\%T$ (percent transmittance of light) versus time was linear up to 60% of the reaction indicating the disappearance of IC follows first order kinetics (**Figure 8**). The rate constant values are tabulated in **Table 3** and the reaction rate decreases with increase in concentration of IC. This is because with increase in the dye concentration, the solution becomes more intensely colour and the path length of the photons entering the solution is decreased thereby few photons reaches the catalyst surface. Hence the production of hydroxyl radicals is reduced. Therefore the photodegradation efficiency is reduced. The pH and *COD* for IC solutions before and after degradation were measured and given in **Table 3**.

To account for the mineralization of dye *COD* was determined at different stage. The formation of different radical species during photodegradation is given in **Scheme 2**. The dye was found to have mineralized into H_2O , CO_2 and simpler inorganic salts [32], after being irradiated for 5 hrs using ZnO/Nb_2O_5 photocatalyst. The photodegradation efficiency of the photocatalyst was calculated by the following formula (**Figure 9**).

$$\text{Photodegradation efficiency} = \frac{\text{Initial } COD - \text{Final } COD}{\text{Initial } COD} \times 100$$

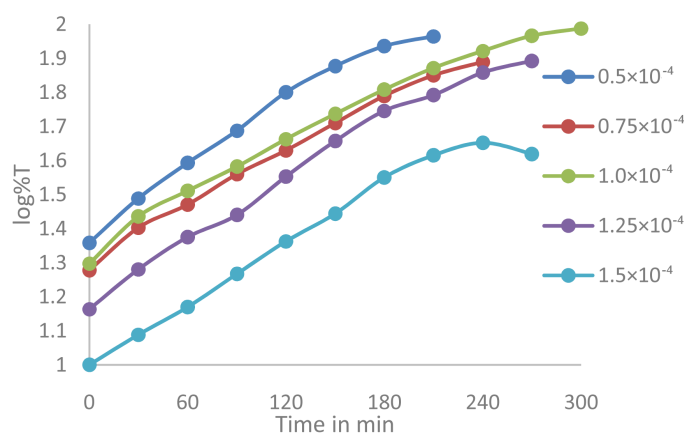


Figure 8. Effect of concentration of IC on the rate of degradation.

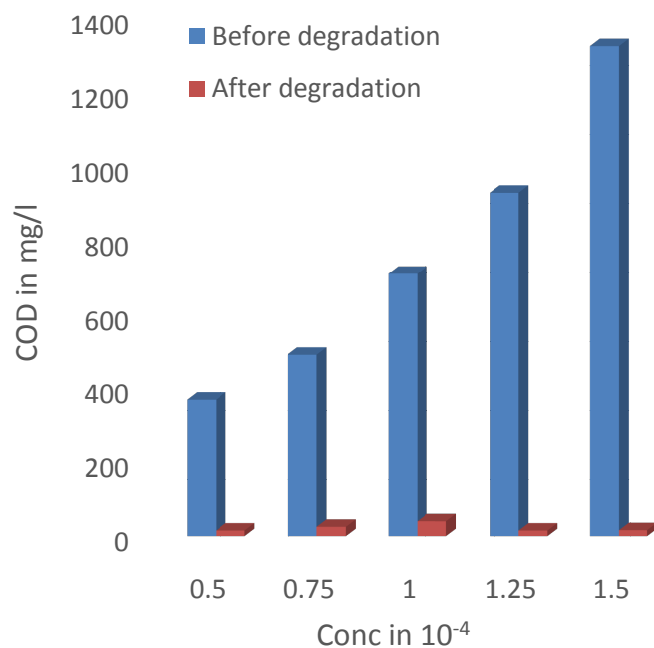
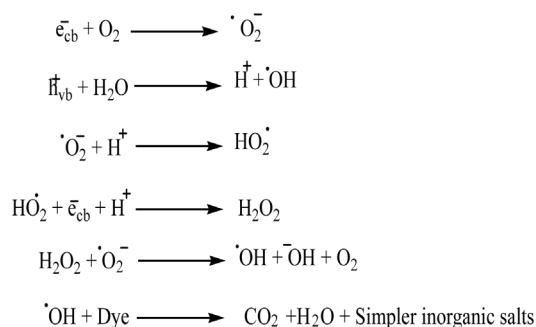


Figure 9. Effect of concentration of IC on COD values.



Scheme 2. Mechanism for the photodegradation of Dye.

Table 3. Effect of photodegradation at different concentration of Indigo carmine.

10^{-4} [IC]	ksec ⁻¹	Effect of pH		COD values in mg/l	
		Before degradation	After degradation	Before degradation	After degradation
0.5	12.1×10^5	6.95	6.14	370	15
0.75	10.1×10^5	7.32	6.89	490	25
1.0	9.67×10^5	7.68	6.93	710	40
1.25	7.61×10^5	7.83	6.82	930	15
1.5	5.81×10^5	7.95	6.75	1327	16

4.2. Effect of pH

The solution pH is an important variable in the evaluation of aqueous phase mediated photocatalytic reactions. The pH of the solution was adjusted by adding 0.001 M HNO₃ or 0.001 M NaOH solution. The effect of pH was studied at pH 7.02, pH 6.02, pH 9.02 and pH 10.02 by keeping all other experimental conditions constant. The results are illustrated in **Figure 10** and tabulated in **Table 4**. The rate of degradation is observed to be slow at lower pH (<7.02) and higher (>9.02) pH. It was observed that the amount of material recovered after the experiment was lowered at lower and higher pH because of the dissolution of semiconductor oxides at extreme pH values. Results of COD effects are illustrated in **Figure 11**. The optimum selected is 10.02 at which photodegradation is high.

4.3. Effect of Catalyst Loading

The experiments were performed by taking different amount of catalyst varying from 3.0 mg to 7.0 mg in order to study the effect of catalyst loading. The study showed that increase in catalyst loading from 3.0 mg - 7.0 mg increased dye removal efficiency. Further increase in catalyst above 7.0 mg decreased the photoactivity of the catalyst, which is due to the aggregation of ZnO/Nb₂O₅ nanoparticles at high concentration causing a decrease in the number of surface active sites and increase in the opacity and light scattering of ZnO/Nb₂O₅ nanoparticles at high concentration. This tends to decrease the passage of light through the sample. Further, in the present study indicated, from economic point of view, the optimized photocatalyst loading is 7.0 mg/20 ml (**Figure 12** and **Table 5**). A result of COD effect is illustrated in **Figure 13**.

4.4. Effect of Light Intensity

The photodegradation rate with UV light is compared with sunlight. It is observed that the photodegradation rate is increased in UV light for prepared photocatalysts compared to ZnO (**Figure 14** and **Figure 15**, **Table 6**). The reason is that, the inclusion of Nb⁵⁺ in ZnO matrix caused an increase in the band gap of ZnO from 3.3 eV to 3.8 eV, indicating that these semiconductor nanoparticles absorb UV light. This can subsequently activate these modified metal oxide photocatalysts upon UV light irradiation. When a photon incident on a semiconductor (ZnO/Nb₂O₅) has energy that matches or exceeds the band gap energy of the semiconductor, an e⁻ is promoted from the valence band (VB) into the conduction band (CB), leaving a hole in the VB. Excited-state CB electrons and VB holes can recombine and dissipate the input energy as heat, get trapped in metastable surface states, or

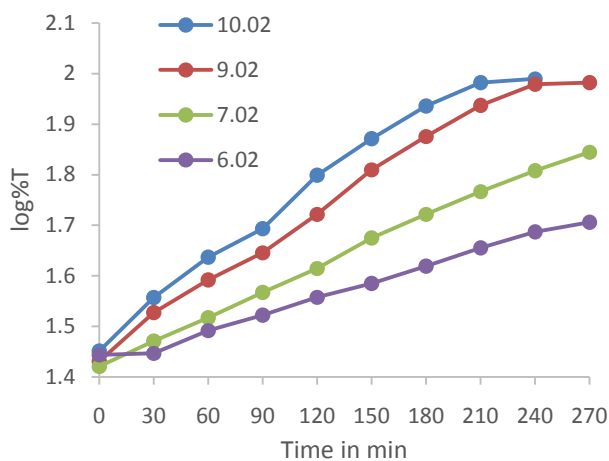


Figure 10. Effect of pH on the rate of degradation of IC.

Table 4. Effect of pH on photodegradation of Indigo carmine.

pH	$k\text{sec}^{-1} \times 10^5$	COD values in mg/l		Photodegradation efficiency %
		Before degradation	After degradation	
6.02	4.47	730	38	94.79
7.02	6.39	730	38	94.79
9.02	9.38	730	16	97.80
10.02	11.0	730	16	97.80

Table 5. Effect of catalyst loading on the photodegradation of IC.

Catalyst ($\text{ZnO}/\text{Nb}_2\text{O}_5$) in mg	$k\text{sec}^{-1}$	Effect of pH		COD in mg/l	
		Before degradation	After degradation	Before degradation	After degradation
3.0	4.51×10^5	7.72	6.51	710	32
4.0	7.63×10^5	7.75	6.72	710	16
6.0	10.4×10^5	7.80	6.83	710	32
7.0	11.1×10^5	7.85	6.95	710	16

Table 6. Effect of photodegradation at different concentration of IC under sunlight.

10^{-4} [IC]	sec^{-1}	Effect of pH		COD values in mg/l	
		Before degradation	After degradation	Before degradation	After degradation
0.5	4.19×10^5	6.97	6.15	370	16
0.75	4.13×10^5	7.34	6.90	490	32
1.0	3.88×10^5	7.68	6.89	710	16
1.25	3.05×10^5	7.82	6.83	930	32
1.5	2.99×10^5	7.91	6.75	1327	32

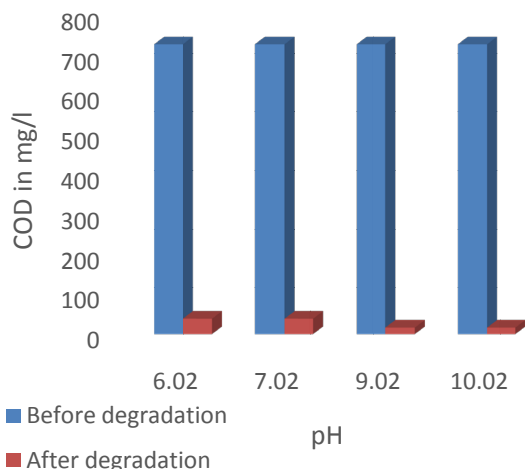


Figure 11. Effect of pH on COD values.

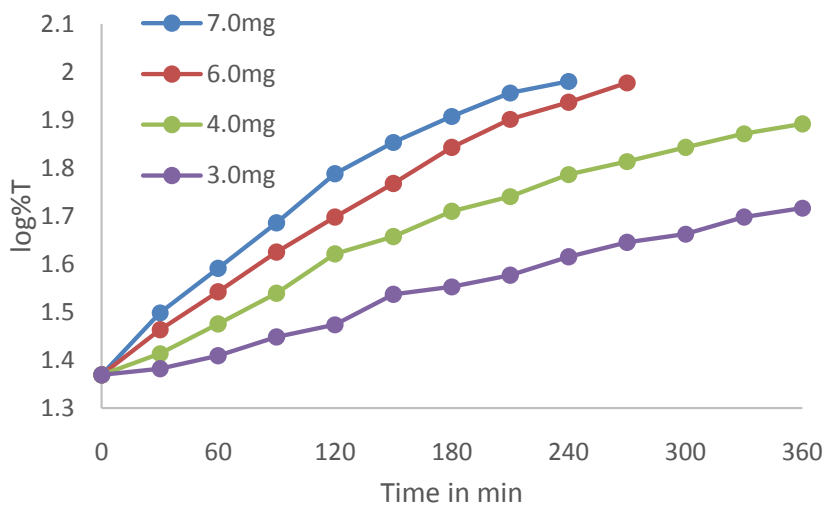


Figure 12. Effect of catalyst loading on photodegradation of IC.

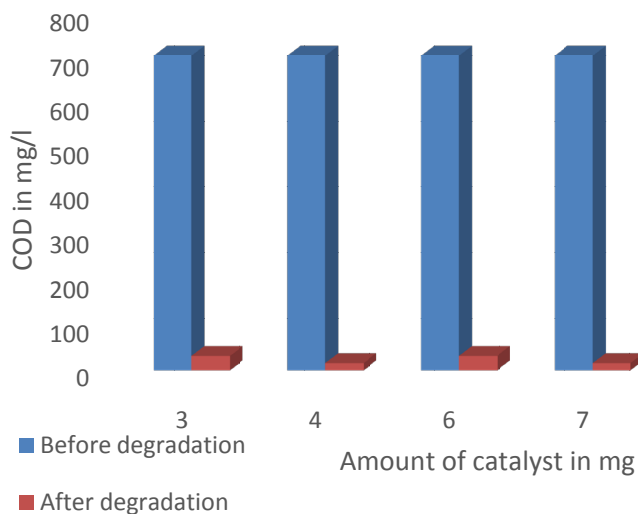


Figure 13. Effect of catalyst loading on COD values for the degradation of IC.

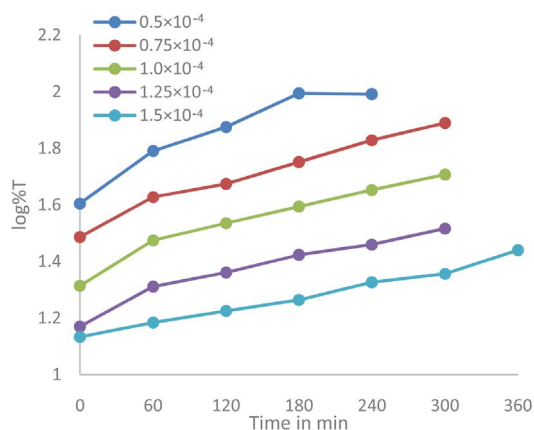


Figure 14. Effect of concentration on IC on the rate of degradation in sunlight.

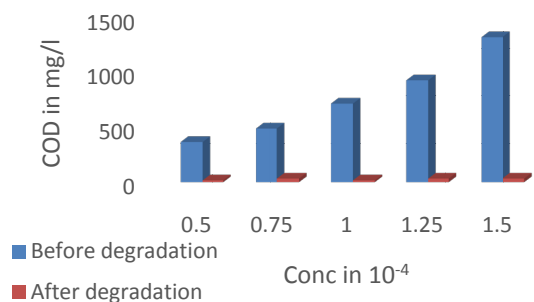


Figure 15. Effect of concentration of IC on COD for the degradation in sunlight.

react, respectively, with electron acceptors and donors that happen to be adsorbed on the semiconductor surface or within the surrounding electrical double layer of the charged nanoparticles. In the absence of suitable e^-/h^+ scavengers the stored energy is dissipated within a few nanoseconds by recombination. If a suitable scavenger or surface defect state is available to trap the electron or hole, recombination is prevented and subsequent redox reactions may occur. As the number of defects in ZnO/Nb₂O₅ nanoparticles, electron or hole recombination is prevented and therefore the ZnO/Nb₂O₅ is very active under UV light compared to bare ZnO.

5. Reuse of the Photocatalyst

The possibility of reusing the photocatalyst was examined to see the cost effectiveness of the method. After the degradation of the dye, the dye solution was kept standing for 10 hrs and then the supernatant was decanted. The photocatalyst was then thoroughly washed with double distilled water and reused for degradation with fresh of dye solution. It was observed that the photocatalytic efficiency was slightly decreased to approximately 80% for the use of second time. Further use of the catalyst showed lesser efficiency.

6. Biological Activities

Niobium doped ZnO nanoparticles synthesised by the electrochemical method were tested for antibacterial activity by Disc diffusion method against different bacteria. The pure bacterial culture was subculture on nutrient agar media. The activity was compared against standard gentamycin (+ve) control and (–ve) control. The solutions was prepared by dissolving 1.0 mg in 100 μ l DMSO and was made up to 1 ml by methanol, which gives the concentration of 1 mg/ml and 30 μ l of each solution was placed on a disc. After incubation for 48 hrs at 37°C, the different levels of zone inhibition in mm around ZnO/Nb₂O₅ nanoparticles was measured which is as shown in **Figure 16** and **Table 7**. Hence ZnO/Nb₂O₅ nanoparticles shows very good inhibition compared to +Ve and –Ve control.

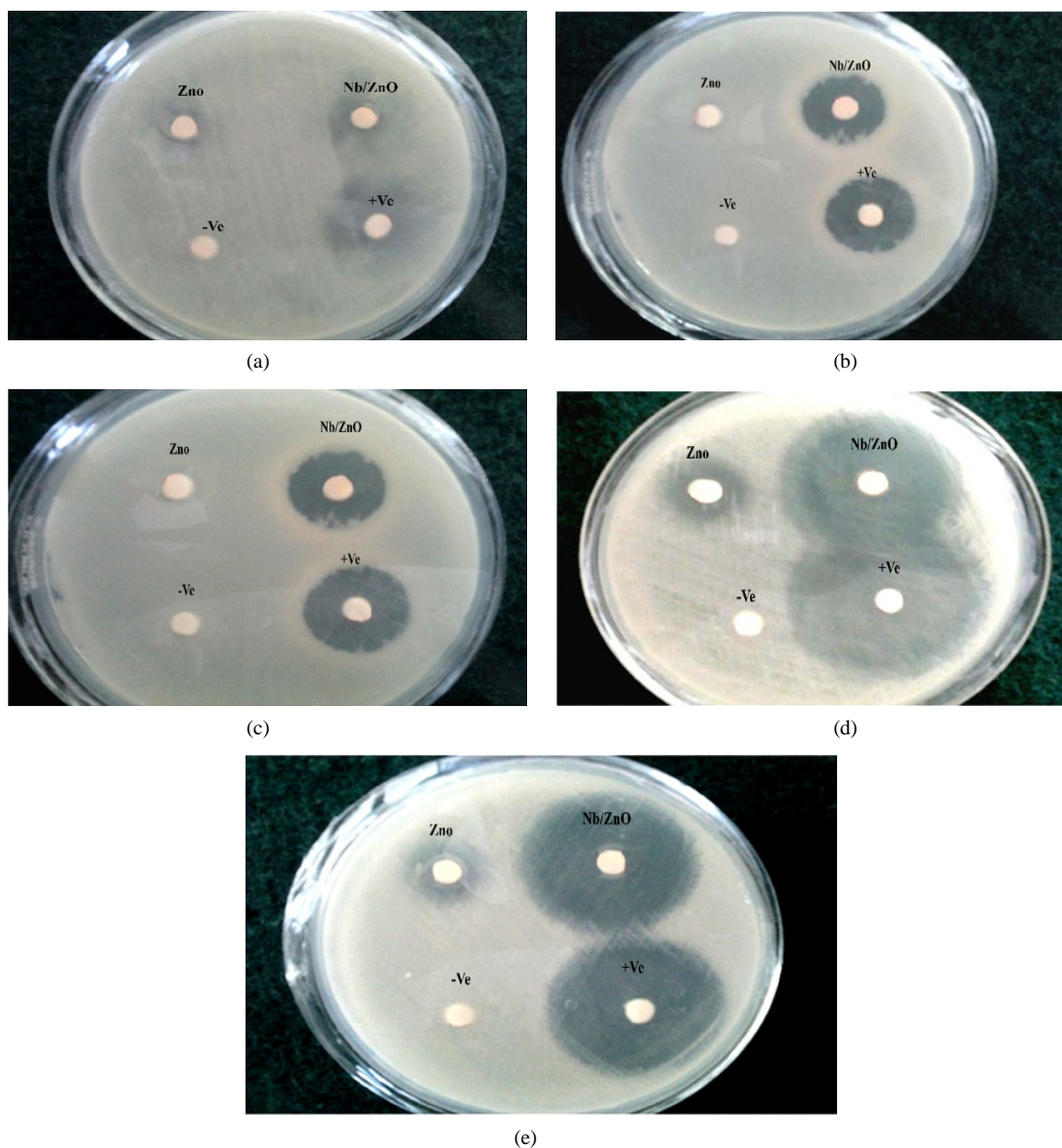


Figure 16. (a) *Escherichia coli*; (b) *Xanthomonas oryzae*; (c) *Salmonella typhii*; (d) *Enterobacter aerogens*; (e) *Pseudomonas aregunosa*.

Table 7. Zone of inhibition (mm) of ZnO/Nb₂O₅ nanoparticles.

Test organisms	ZnO	ZnO/Nb ₂ O ₅	+Ve	-Ve
<i>Escherichia coli</i>	0.9	1.9	2.1	0
<i>Xanthomonas oryzae</i>	0.4	1.0	1.2	0
<i>Salmonella typhii</i>	0.5	0.8	1.0	0
<i>Enterobacter aerogens</i>	0.8	1.9	2.2	0
<i>Pseudomonas aregunosa</i>	0.4	0.7	1.0	0

7. Conclusion

ZnO/Nb₂O₅ nanoparticles were synthesised by electrochemical method an environment friendly method. These

nanoparticles were characterised by UV, IR, SEM, XRD, ICPMS and EDAX analysis. Photodegradation by these semiconductors offers a green technology for the removal of hazardous compounds present in the industrial effluents. Kinetics for the degradation of indigocarmine by ZnO/Nb₂O₅ nanoparticles were studied systematically. The completion of degradation was confirmed by COD experiment. Results of COD revealed that ~96% of the dye had been degraded. These nanoparticles act as a very good catalyst for the degradation of dye and a promising antibacterial agent.

References

- [1] Djuricic, A.B. (2002) Progress in the Room-Temperature Optical Functions of Semiconductors. *Materials Science and Engineering: R: Reports*, **38**, 237-293. [http://dx.doi.org/10.1016/S0927-796X\(02\)00063-3](http://dx.doi.org/10.1016/S0927-796X(02)00063-3)
- [2] Dong, L.F., Jiao, J., Tuggle, D.W., Petty, L.M. and Elliff, S.A. (2003) ZnO Nanowires Formed on Tungsten Substrates and Their Electron Field Emission Properties. *Applied Physics Letters*, **82**, 1096-1098. <http://dx.doi.org/10.1063/1.1554477>
- [3] Zhu, B.L., Xie, C.S., Wang, A.H., Wu, J., Wu, R. and Liu, J. (2007) Laser Sintering ZnO Thick Films for Gas Sensor Application. *Journal of Materials Science*, **42**, 5416-5420. <http://dx.doi.org/10.1007/s10853-006-0768-2>
- [4] Agarwal, G. and Speyer, R.F. (1998) Current Change Method of Reducing Gas Sensing Using ZnO Varistors. *Journal of Electrochemical Society*, **145**, 2920-2925. <http://dx.doi.org/10.1149/1.1838737>
- [5] Kind, H., Yan, H., Messer, B., Law, M. and Yang, P. (2002) Nanowire Ultraviolet Photodetectors and Optical Switches. *Advanced Materials*, **14**, 158-160. [http://dx.doi.org/10.1002/1521-4095\(20020116\)14:2<158::AID-ADMA158>3.0.CO;2-W](http://dx.doi.org/10.1002/1521-4095(20020116)14:2<158::AID-ADMA158>3.0.CO;2-W)
- [6] Byrappa, K., Subramani, A.K., Ananda, S., Lakanatharai, K.M., Sunitha, M.H., Basavalingu, B. and Soga, K. (2006) Impregnation of ZnO onto Activated Carbon under Hydrothermal Conditions and Its Photocatalytic Properties. *Journal of Materials Science*, **41**, 1355-1362. <http://dx.doi.org/10.1007/s10853-006-7341-x>
- [7] Xu, F., Zhang, P., Navrotsky, A., Yuan, Z.Y., Ren, T.Z., Halasa, M. and Su, B.L. (2007) Hierarchically Assembled Porous ZnO Nanoparticles: Synthesis, Surface Energy, and Photocatalytic Activity. *Chemistry of Materials*, **19**, 5680-5686. <http://dx.doi.org/10.1021/cm071190g>
- [8] Cernigoj, U., Stangar, U.L., Trebse, P., Krasovec, U.O. and Gross, S. (2006) Photocatalytically Active TiO₂ Thin Films Produced by Surfactant-Assisted Sol-Gel Processing. *Thin Solid Films*, **495**, 327-332. <http://dx.doi.org/10.1016/j.tsf.2005.08.240>
- [9] Yu, H., Zhang, K. and Rossi, C. (2007) Theoretical Study on Photocatalytic Oxidation of VOCs Using Nano-TiO₂ Photocatalyst. *Journal of Photochemistry and Photobiology A*, **188**, 65-83. <http://dx.doi.org/10.1016/j.jphotochem.2006.11.021>
- [10] Lizama, C., Freer, J., Baeza, J. and Mansilla, H.D. (2002) Optimized Photodegradation of Reactive Blue 19 on TiO₂ and ZnO Suspensions. *Catalysis Today*, **76**, 235-246. [http://dx.doi.org/10.1016/S0920-5861\(02\)00222-5](http://dx.doi.org/10.1016/S0920-5861(02)00222-5)
- [11] Peng, F., Wang, H., Yu, H. and Chen, S. (2006) Preparation of Aluminum Foil-Supported Nano-Sized, ZnO and Its Photocatalytic Phenol under Visible Light Irradiation. *Materials Research Bulletin*, **41**, 2123-2129. <http://dx.doi.org/10.1016/j.materresbull.2006.03.029>
- [12] Ahmadipour, M., Hatami, M. and Rao, K.V. (2012) Preparation and Characterization of Nano-Sized (Mg_xFe_(1-x)O/SiO₂) (x=0.1) Core-Shell Nanoparticles by Chemical Precipitation Method. *Advances in Nanoparticles*, **1**, 37-43.
- [13] Qiu, X.Q., Li, G.S., Sun, X.F., Li, L.P. and Fu, X.Z. (2008) Doping Effects of Co²⁺ Ions on ZnO Nanorods and Their Photocatalytic Properties. *Nanotechnology*, **19**, Article ID: 215703. <http://dx.doi.org/10.1088/0957-4484/19/21/215703>
- [14] Marci, G., Augugliaro, V., López-Muñoz, M.J., Martin, C., Palmisano, L., Rives, V., Schiavello, M., Tilley, R.J.D. and Venezia, A.M. (2001) Preparation Characterization and Photocatalytic Activity of Polycrystalline ZnO/TiO₂ Systems. 2. Surface, and Bulk Characterization, and 4-Nitrophenol Photodegradation in Liquid-Solid Regime. *Journal of Physical Chemistry B*, **105**, 1033-1040. <http://dx.doi.org/10.1021/jp003173j>
- [15] Ullah, R. and Dutta, J. (2008) Photocatalytic Degradation of Organic Dyes with Manganese-Doped ZnO Nanoparticles. *Journal of Hazardous Materials*, **156**, 194-200. <http://dx.doi.org/10.1016/j.jhazmat.2007.12.033>
- [16] Zhang, Q., Fan, W. and Gao, L. (2007) Anatase TiO₂ Nanoparticles Immobilized on ZnO Tetrapods as a Highly Efficient and Easily Recyclable Photocatalyst. *Applied Catalysis B: Environmental*, **76**, 168-173. <http://dx.doi.org/10.1016/j.apcatb.2007.05.024>
- [17] Anandan, S., Vinu, A., Lovely, K.L.P.S., Gokulakrishnan, N., Srinivasu, P., Mori, T., Murugesan, V., Sivamurugan, V. and Ariga, K. (2007) Photocatalytic Activity of La-Doped ZnO for the Degradation of Monocrotophos in Aqueous Suspension. *Journal of Molecular Catalysis A: Chemical*, **266**, 149-157. <http://dx.doi.org/10.1016/j.molcata.2006.11.008>
- [18] Li, D. and Haneda, H. (2003) Photocatalysis of Sprayed Nitrogen-Containing Fe₂O₃-ZnO and WO₃-ZnO Composite

- Powders in Gas-Phase. *Journal of Photochemistry and Photobiology A: Chemistry*, **160**, 203-212. [http://dx.doi.org/10.1016/S1010-6030\(03\)00212-0](http://dx.doi.org/10.1016/S1010-6030(03)00212-0)
- [19] Ekambaram, S., Likubo, Y. and Kudo, A. (2007) Combustion Synthesis and Photocatalytic Properties of Transition Metal-Incorporated ZnO. *Journal of Alloys and Compounds*, **433**, 237-240. <http://dx.doi.org/10.1016/j.jallcom.2006.06.045>
- [20] Lin, H.F., Liao, S.C. and Hung, S.W. (2005) The dc Thermal Plasma Synthesis of ZnO Nanoparticles for Visible-Light Photocatalyst. *Journal of Photochemistry and Photobiology A: Chemistry*, **174**, 82-87. <http://dx.doi.org/10.1016/j.jphotochem.2005.02.015>
- [21] Nyffenegger, R.M., Craft, B., Shaaban, M., Gorer, S., Erley, G. and Penner, R.M. (1998) A Hybrid Electrochemical/Chemical Synthesis of Zinc Oxide Nanoparticles and Optically Intrinsic Thin Films. *Chemistry of Materials*, **10**, 1120-1129. <http://dx.doi.org/10.1021/cm970718m>
- [22] Therese, G.H.A. and Kamath, P.V. (2000) Electrochemical Synthesis of Metal Oxides and Hydroxides. *Chemistry of Materials*, **12**, 1195-1204. <http://dx.doi.org/10.1021/cm990447a>
- [23] Byrappa, K., Subramani, A.K., Ananda, S., Rai, K.M.L., Dinesh, R. and Yoshimura, M. (2006) Photocatalytic Degradation of Rhodamine B Dye Using Hydrothermally Synthesized ZnO. *Bulletin of Materials Science*, **29**, 433-438. <http://dx.doi.org/10.1007/BF02914073>
- [24] Belever, C., Adán, C. and Fernández-García, M. (2009) Photocatalytic Behaviour of Bi₂MO₆ Polymetalates for Rhodamine B Degradation. *Catalysis Today*, **143**, 274-281. <http://dx.doi.org/10.1016/j.cattod.2008.09.011>
- [25] Carp, O., Huisman, C.L. and Rellar, A. (2004) Photoinduced Reactivity of Titanium Dioxide. *Progress in Solid State Chemistry*, **32**, 33-177. <http://dx.doi.org/10.1016/j.progsolidstchem.2004.08.001>
- [26] Sclafani, A. and Hermann, J.M. (1998) Influence of Metallic Silver and of Platinum-Silver Bimetallic Deposits on the Photocatalytic Activity of Titania (Anatase and Rutile) in Organic and Aqueous Media. *Journal of Photochemistry and Photobiology A: Chemistry*, **113**, 118-188. [http://dx.doi.org/10.1016/S1010-6030\(97\)00319-5](http://dx.doi.org/10.1016/S1010-6030(97)00319-5)
- [27] Rodriguez, J.A. and Fernández-García, M. (2007) Synthesis Properties and Applications of Oxide Nanomaterials. John Wiley and Sons, Inc., New York, 335-351. <http://dx.doi.org/10.1002/0470108975>
- [28] Li, X., Han, X., Wang, W., Liu, X., Wang, Y. and Liu, X. (2012) Synthesis, Characterization and Photocatalytic Activity of Nb-Doped TiO₂ Nanoparticles. *Advanced Materials Research*, **455**, 110-111.
- [29] Lakshmi, G.C., Ananda, S., Somashekar, R. and Ranganathaiah, C. (2012) Synthesis of ZnO/MgO Nanocomposites by Electrochemical Method for Photocatalytic Degradation Kinetics of Eosin Yellow Dye. *International Journal of Nano-Science and Nanotechnology*, **3**, 47-63.
- [30] Patil, A.V., Dighavkar, C.G., Sonawane, S.K., Patil, S.J. and Borse, R.Y. (2010) Influence of Nb₂O₅ Doping on ZnO Thick Film Gas Sensors. *Journal of Optoelectronics and Advanced Materials*, **12**, 125-1261.
- [31] Pail, D.R., Patil, L.A. and Amalnerkar, D.P. (2007) Ethanol Gas Sensing Properties of Al₂O₃-Doped ZnO Thick Film Resistors. *Bulletin of Materials Science*, **30**, 553-559. <http://dx.doi.org/10.1007/s12034-007-0086-6>
- [32] Wei, L., Shifu, C., Wei, Z. and Sujuan, Z. (2009) Titanium Dioxide Mediated Photocatalytic Degradation of Mathamiodophos in Aqueous Phase. *Journal of Hazardous Materials*, **164**, 154-160. <http://dx.doi.org/10.1016/j.jhazmat.2008.07.140>

Scientific Research Publishing (SCIRP) is one of the largest Open Access journal publishers. It is currently publishing more than 200 open access, online, peer-reviewed journals covering a wide range of academic disciplines. SCIRP serves the worldwide academic communities and contributes to the progress and application of science with its publication.

Other selected journals from SCIRP are listed as below. Submit your manuscript to us via either submit@scirp.org or [Online Submission Portal](#).

